JOURNAL OF NEUROTRAUMA 36:2129–2138 (July 1, 2019)

DOI: 10.1089/neu.2018.6291

A Role for Postsynaptic Density 95 and Its Binding Partners in Models of Traumatic Brain Injury

Mihir V. Patel,[1,2] Emily Sewell,[3] Samantha Dickson,[3] Hyuck Kim,[1] David F. Meaney,[3] and Bonnie L. Firestein[1]

Abstract

Postsynaptic density 95 (PSD-95), the major scaffold protein at excitatory synapses, plays a major role in mediating intracellular signaling by synaptic *N*-methyl-D-aspartate (NMDA) type glutamate receptors. Despite the fact that much is known about the role of PSD-95 in NMDA-mediated toxicity, less is known about its role in mechanical injury, and more specifically, in traumatic brain injury (TBI). Given that neural circuitry is disrupted after TBI and that PSD-95 and its interactors end-binding protein 3 (EB3) and adenomatous polyposis coli (APC) shape dendrites, we examined whether changes to these proteins and their interactions occur after brain trauma. Here, we report that total levels of PSD-95 and the interaction of PSD-95 with EB3 increase at 1 and 7 days after moderate controlled cortical impact (CCI), but these changes do not occur after mild injury. Because changes occur to PSD-95 following brain trauma *in vivo*, we next considered the functional consequences of PSD-95 alterations *in vitro*. Rapid deformation of cortical neurons leads to neuronal death 72 h after injury, but this outcome is not dependent on PSD-95 expression. However, disruptions in dendritic arborization following stretch injury *in vitro* require PSD-95 expression, and these changes in arborization can be mimicked with expression of PSD-95 mutants lacking the second PDZ domain. Thus, PSD-95 and its interactors may serve as therapeutic targets for repairing dendrites after TBI.

Keywords: APC; CCI; dendrite morphology, EB3; mechanical injury; PSD-95; stretch-induced injury; TBI

Introduction

Traumatic brain injury (TBI) is caused by the rapid movement of the brain within the skull, leading to neuronal damage and injury to the brain. A traumatic event can be an impact, such as direct contact with an object, or non-impact, such as an indirect blast or acceleration. In the United States, TBI leads to 56,000 deaths per year.[1] Falls, vehicle accidents, sports-related concussions,[2] and blast injury in military individuals[3] are the leading causes of TBI in the United States.

Primary brain insult occurs immediately after trauma and includes mechanical damage to blood vessels, neurons, and glia. Secondary insult is the indirect result of the events initiated by the primary brain injury and occurs from hours to weeks after trauma.[4] Secondary insult involves glutamate-mediated excitotoxicity and increased calcium influx, promoting synaptic dysfunction, dendrite and axon degeneration, and, ultimately, neuronal death.[4,5] Downstream signaling cascades activated by increased calcium influx from *N*-methyl-D-aspartate (NMDA) receptors cause damage to dendrites,[6] resulting in short-term cognitive deficits after mild TBI,[7] and long-term or permanent cognitive deficits and disabilities after moderate to severe TBI.[8] As of yet, no treatment is available to either prevent or treat secondary insult. Many NMDA receptor antagonist drugs and neuroprotective agents have failed to promote cognitive improvement after TBI in clinical trials.[9,10] Therefore, the unavailability of a promising therapeutic approach motivates the study of detailed molecular mechanisms involved in short- and long-term changes or deficits after TBI.

Possible therapeutic targets for recovery after TBI include pathways involved in the reconnection of neural circuitry. For example, reestablishment of the dendritic network is required for proper neuronal signaling and improvement of cognitive function. Although a number of studies have focused on axonal degeneration following TBI,[11–13] less attention has been given to the effects of TBI on dendritic arborization.[14] Understanding mechanisms underlying the development and maintenance of dendritic arborization will help to develop new therapeutic approaches for the recovery of cognitive function and identify new molecular targets for the development of novel drugs and therapeutic approaches for the treatment of TBI.

Postsynaptic density-95 (PSD-95), one such molecular target, is the major scaffolding protein in the postsynaptic density (PSD) of dendritic spines[15–20] and is essential for glutamate-mediated excitotoxicity.[21,22] Overexpression of PSD-95 exacerbates neuronal excitotoxicity mediated by NMDA glutamate type receptors, and knockdown attenuates neuronal death.[23] Further, overexpression

[1]Department of Cell Biology and Neuroscience, [2]Graduate Program in Neurosciences, Rutgers University, Piscataway, New Jersey.
[3]Department of Bioengineering, University of Pennsylvania, Philadelphia, Pennsylvania.

of PSD-95 in cultured hippocampal neurons promotes maturation of spines.[24] In addition to its function in spines, PSD-95 restricts dendritic arborization by binding to a proline-rich region in the plus-end tracking proteins (+TIP) microtubule end-binding protein 3 (EB3) through its SRC Homology 3 (SH3) domain.[25,26] Additionally, interaction between PSD-95 and another +TIP binding protein, adenomatous polyposis coli (APC),[27] results in stimulation of microtubule assembly, bundling, and stabilization.[28,29] APC regulates microtubules at branch points[30] and mediates neurite outgrowth.[31–33] Therefore, targeting PSD-95 levels and interactions with binding partners may be of therapeutic value for repair of neural circuits, and specifically dendrite morphology, after TBI.

In the current study, we used both *in vitro* and *in vivo* models to assess the role of PSD-95 and its interaction with binding partners in TBI. We found that moderate TBI increases PSD-95 levels and interaction with APC and EB3 at 1 and 7 days after controlled cortical impact (CCI), and levels return to baseline by 14 days. In comparison, we observed no significant change in either PSD-95 or its binding partner associations following mild cortical impact injury. Together these data suggest that remodeling mechanisms after TBI differ depending on injury severity. Based on the possibility that PSD-95 and its interactors may play a role in the remodeling process after injury, we knocked down PSD-95 in cultured rat cortical neurons. We found that this knockdown prevents decreases in secondary dendrite number and total dendrite length after stretch-mediated injury, and that PSD-95 must be present for stretch-mediated injury to decrease dendrites. Thus, targeting PSD-95 and its interactions with microtubule-associated proteins may serve as a therapeutic strategy after TBI.

Methods

All animal experiments were conducted in accordance with the National Institutes of Health (NIH) Guide for the Care and Use of Laboratory animals (NIH Publication No. 8023, revised 1978).

CCI

Animals were injured using the CCI model.[34,35] Adult male mice (C57BL/6J; #000664; 23–29g; Jackson Laboratory) were anesthetized with isoflurane (5% induction, 1–2% maintenance) and placed into a stereotactic frame. A 1.0 cm midline rostral-to-caudal incision was made, and a craniotomy was performed over the left parietotemporal cortex midway between bregma and lambda 2.5 mm lateral to the sagittal suture. The dura was kept intact. One hour after induction of anesthesia, a spherical 2 mm diameter indentor tip was brought slowly down until it contacted the cortical brain surface and retracted into a pull-type solenoid. The indentation depth (1 mm) was adjusted using a micrometer, and the solenoid was energized to deliver an impact at the desired velocity (mild: 0.4–0.5 m/sec; moderate: 4.0–5.0 m/sec). Sham injury included craniotomy only.

Western blot analysis

Western blot analysis was performed as previously described.[36] Rat brain, cortical tissue, or cultured cortical neurons were homogenized in RIPA buffer (50 mM Tris-HCl, pH 7.4, 150 mM NaCl, 0.5% deoxycholate, 1% NP-40, 0.1% sodium dodecyl sulfate (SDS), 1 mM ethylenediaminetetraacetic acid (EDTA), pH 7.4). Protein concentrations were determined using the Pierce BCA protein assay kit (Thermo Scientific) following the manufacturer's protocol. Proteins (15 μg) were resolved on a 10% SDS-polyacrylamide gel and transferred to polyvinylidene difluoride (PVDF) membrane. The membrane was blocked with 5% bovine serum albumin (BSA) in TBST (20 mM Tris pH 7.5, 150 mM NaCl, 0.1% Tween-20) for 1 h. The blot was probed with indicated antibodies in TBST containing 3% BSA: mouse anti-PSD-95 (1:1000; K28/43, UC Davis/NIH NeuroMab Facility), rabbit anti-APC (1:250; SC-20, Santa Cruz Biotech.; 1:100; Ab15270, Abcam), mouse anti-GAPDH (1:1000; MAB374, Millipore), and rabbit anti-EB3 (BF4[26]). Blots were scanned, and the intensities of bands were quantified using ImageJ software (NIH). The number of pixels of absolute intensity of bands was normalized to the intensity of those for glyceraldehyde 3-phosphate dehydrogenase (GAPDH) (internal control) and was compared with that of the control condition.

Co-immunoprecipitation (co-IP)

For co-IP experiments, total protein extract from 0.9 mg of cortical tissue was used for each IP. Mouse anti-PSD-95 (K28/43, UC Davis/NIH NeuroMab Facility) or normal mouse immunoglobulin (Ig)G (5 μg) was added to the extracts, and the extracts were incubated overnight at 4°C. Protein A Sepharose beads (30 μl; GE Healthcare) were added, and the extracts were incubated for 1 h at 4°C. Beads were washed three times with TEE buffer (20 mM Tris-HCl, pH 7.4, 1mM EDTA, 1 mM egtazic acid [EGTA], pH 7.4), and immunoprecipitated proteins were eluted into 25μl 2 × SDS- polyacrylamide gel electrophoresis (PAGE) sample buffer (0.02 M Tris-HCl, pH 6.8, 40% glycerol, 20% β-mercaptoethanol, 4.6% SDS, 0.01% bromophenol blue) and boiled for 5 min followed by centrifugation. The supernatant, containing immunoprecipitated proteins, and the initial extract (load) were resolved and Western blot was performed as described in the section *Western blot analysis*. The band intensities of immunoprecipitated PSD-95 and co-immunoprecipitated APC and EB3 were normalized to their respective band intensities in the load. The ratio of normalized intensities of PSD-95 and APC or EB3 from CCI or stretch-mediated injury was compared with that of sham control. Band intensities of all three proteins were normalized to those of GAPDH and compared with those of sham control. Statistical differences ($p < 0.5$) were evaluated by analysis of variance (ANOVA) followed by Tukey's multiple comparisons test using GraphPad Prism7 software. For immunoprecipitation of APC, 1 mg of whole rat brain lysate was used to pull down APC (C-20, Santa Cruz Biotech.) followed by Western blot analysis and probing for APC and PSD-95 as discussed previously.

Neuronal culture

Cortical and hippocampal neuronal cultures were prepared from rat embryos at 18–19 days gestation, as we have described previously.[25,26,37–41] Neurons were cultured in Neurobasal medium supplemented with B27 and GlutaMax (ThermoFisher Scientific). Hippocampal neurons plated on glass cover-slips coated with Poly-D-Lysine (PDL; 0.1 mg/mL, Sigma) were used to study the role of PDZ domains of PSD-95 in the regulation of dendrite branching. Cortical neurons were plated at a density of 105 cells/cm^2 on stretchable elastomeric silicone membranes (SMI Inc.; Gloss 0.01'' thick, 40 Durometer) that were coated overnight with PDL (0.1 mg/mL, Sigma) and laminin (0.002 mg/mL, Sigma) in a 37°C incubator with 5% CO_2 for stretch-mediated injury experiments. Silastic membranes were pre-stretched to 142.8% of their original width.[42–44]

Mechanical stretch injury

Cultured cortical neurons grown on flexible membranes were placed into a sealed stretch injury chamber.[42–44] Pressurized air was applied at 20 psi (consistent output pressure of 12 psi) for 50 ms. The membrane in the injured region was stretched uniaxially, where the width was extended to 60% beyond the initial width before returning to the original dimensions. Naive unstretched neurons were used as uninjured controls.

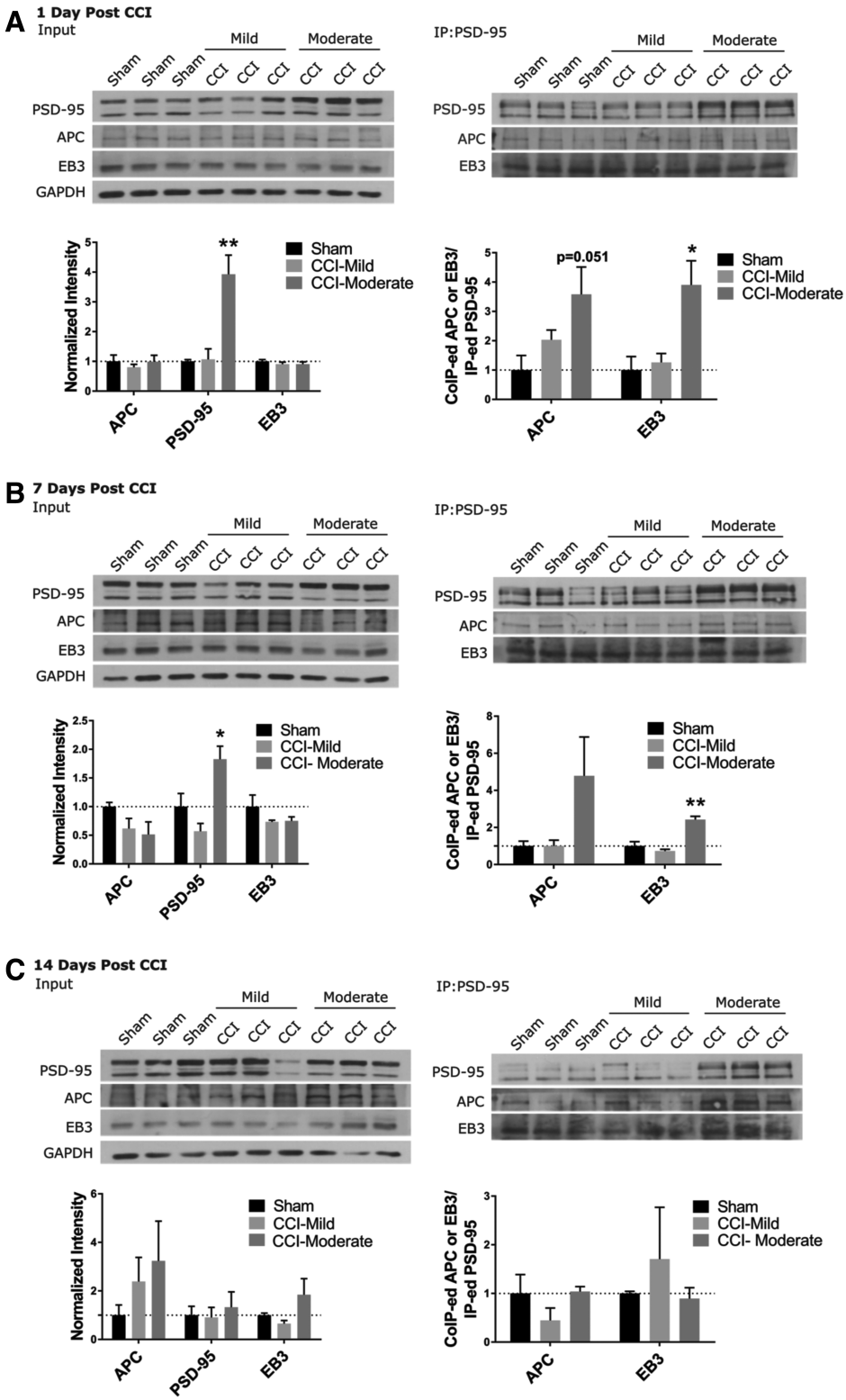

FIG. 1. Expression of postsynaptic density 95 (PSD-95) and interaction with adenomatous polyposis coli (APC) and end-binding protein 3 (EB3) change differently in mice subjected to mild or moderate controlled cortical impact (CCI). PSD-95 was immunoprecipitated from extracts from cortices of mice exposed to sham injury or CCI. Lysates and immunoprecipitates were subjected to Western blot analysis. **(A)** Western blots and densitometric analysis for cortices at 1 day after mild and moderate injury. **(B)** Western blots and densitometric analysis for cortices at 7 days after mild and moderate injury. **(C)** Western blots and densitometric analysis for cortices at 14 days after mild and moderate injury. $n = 3$–4 mice for each time point. $^{*}p < 0.05$ and $^{**}p < 0.01$ as determined by comparing CCI with sham condition using one way analysis of variance (ANOVA) followed by Dunnett's multiple comparisons test except for the use of Student's t test followed by Welch's correction for 2 h after mild injury. Error bars = SEM.

shRNA and lentivirus production

Lentivirus was produced as previously described.[36,45] Scramble (Target sequence – CCTAAGGTTAAGTCGCCCTCG; VectorBuilder) and PSD-95 shRNA (Target sequence in ORF – ACGATC ATCGCTCAGTATAAA; VectorBuilder) lentivirus were used in this study. In brief, on day 1, HEK293T cells were plated at a density of 6.5×10^6 cells/T75 flask. On day 2, cells were transfected with lentiviral plasmid and PAX2 and VSV packaging vectors using Lipofectamine 2000 reagent (Invitrogen) following the manufacturer's protocol. On day 5, supernatant was collected and centrifuged at 1500*g* for 5 min to remove dead cells and debris. The supernatant was transferred into a new tube containing 5×PEG-it™ virus precipitation solution (System Biosciences; 1:4 dilution), followed by incubation at 4°C for 2 days to concentrate the virus. On day 7, the mixture was centrifuged at 1500*g* for 30 min at 4°C to pellet the virus. The supernatant was carefully removed, and the pellet was resuspended in 150–200 μL sterile phosphate-buffered saline (PBS) and aliquoted into 10 μL fractions, which were stored at −80°C until further use.

Neuronal survival assay

Neurons were transduced on day *in vitro* (DIV) 11 with scramble or PSD-95 shRNA lentivirus. Neurons were mechanically injured on DIV 14, followed by fixation on DIV 17 with 4% paraformaldehyde (PFA) in PBS and immunostaining with mouse anti-MAP2 (1:250; BD PharMingen). MAP2-positive neurons were counted to determine neuronal viability. Ten random regions observed under 10×objective were selected and imaged, and the average number of MAP2-positive neurons was counted for each condition.

Sholl analysis

Hippocampal neurons were co-transfected with cDNA encoding monomeric red fluorescent protein (mRFP) and green fluorescent protein (GFP) or GFP-tagged PSD-95, PSD-95ΔPDZ1, PSD-95ΔPDZ2, or PSD-95ΔPDZ3 on DIV 7 to analyze on DIV 12 to study the role of PDZ regions of PSD-95 on dendrite branching.

To study the effect of stretch injury on dendrite branching, cultured cortical neurons were transfected with pGW1-mRFP on DIV 7 using Lipofectamine LTX+PLUS reagent (Invitrogen) following the manufacturer's protocol. Neurons were then transduced on DIV 11 with scramble or PSD-95 shRNA lentivirus. Neurons were mechanically injured on DIV 14 and fixed on DIV 17 with PFA. Cells were then immunostained with chicken anti-GFP (1:250; ThermoFisher) and mouse anti-MAP2 (1:250; BD PharMingen). Immunostaining was visualized with Alexa Fluor 488 and 647 conjugated secondary antibodies (ThermoFisher Sci.). Imaging was performed using an EVOS-FL fluorescence imaging system (ThermoFisher Sci.). All images were analyzed using ImageJ software (NIH) and MATLAB (MathWorks). Sholl analysis was performed using the Bonfire program developed by the Firestein laboratory.[46,47] In brief, concentric circles were drawn around the soma at every 6 μm, and intersections with MAP-2-positive dendrite branches were counted. All data were exported from MATLAB to Excel for quantification. Statistical differences ($p < 0.5$) were determined by two way ANOVA followed by Tukey's multiple comparisons test using GraphPad Prism7 software. The experimenter was blinded to conditions during all Sholl and data analyses.

Results

Mild and moderate CCI result in distinct changes to PSD-95 and EB3

We used CCI as an *in vivo* model of injury to first assess changes to PSD-95 over time following either mild or moderate brain trauma. We observed no significant change in either total levels of PSD-95 or its binding partners EB3 and APC at any time point following mild brain trauma (Fig. 1 A–C, left panels). Because mild TBI and moderate TBI activate different cellular mechanisms,[48] we assessed changes to protein levels in mice exposed to moderate CCI. Unlike in mild brain injury, we observed that total levels of PSD-95 increased at 1 day and 7 days post-moderate CCI (Fig. 1 A,B, left panels). Further, we did not observe significant changes in total expression of either EB3 or APC at any of the examined time points. Our data suggest that PSD-95 may play a role in mediating the effects of moderate brain trauma.

Knockdown of PSD-95 does not protect neurons after stretch-induced injury

Given these changes in PSD-95 after traumatic brain injury *in vivo*, we then explored the functional consequences of altering PSD-95 after mechanical trauma *in vitro*. Our first functional measure was neuronal survival, as this is a key measure in many models of neurological disease and injury. We previously reported

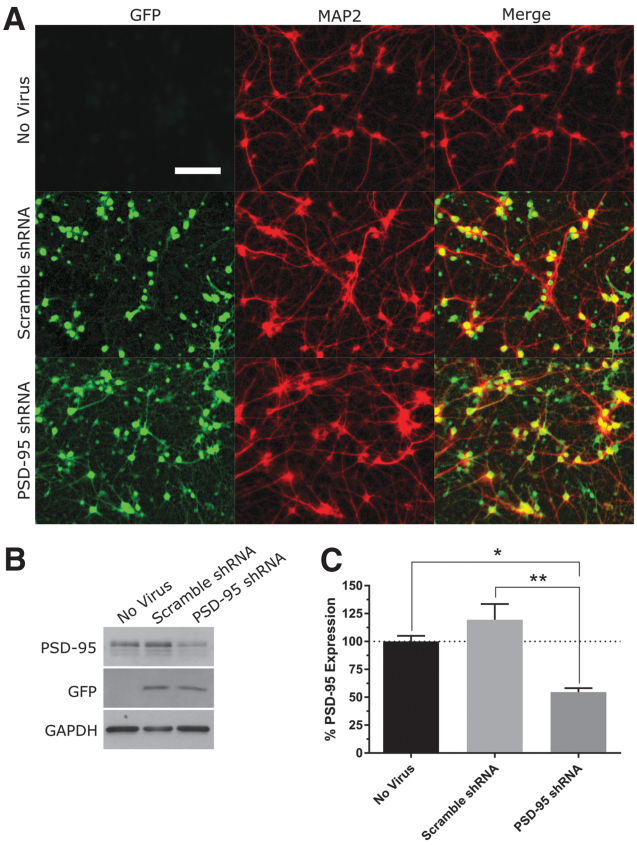

FIG. 2. Postsynaptic density 95 (PSD-95) shRNA decreases PSD-95 protein levels by 50%. **(A)** Representative images of neurons transduced with lentivirus encoding scramble shRNA (control) and green fluorescent protein (GFP) or PSD-95 shRNA on day *in vitro* (DIV) 11 and fixed on DIV 17. Neurons were immunostained for GFP (green) and MAP2 (red). Transduction efficiency is almost 100%. **(B)** Western blot showing GFP and PSD-95 expression in cortical neurons transduced with scramble shRNA or PSD-95 shRNA. **(C)** Quantification of PSD-95 knockdown. $*p < 0.05$; $**p < 0.01$ as determined by one way analysis of variance (ANOVA) followed by Tukey's multiple comparisons test. $n = 3$. Error bars = SEM. Scale bar = 100 μm.

that knockdown of PSD-95 protects neurons from NMDA-induced excitotoxicity[23]; however, it is not known whether PSD-95 knockdown rescues neurons from mechanical injury. We created viruses containing scramble control shRNA and shRNA targeting PSD-95. Scrambled shRNA had no effect on PSD-95 levels, whereas PSD-95 shRNA decreased levels by 50% in cultured neurons transduced with virus (Fig. 2). We then assessed neuronal survival after stretch injury *in vitro*. In control (scramble shRNA) cultures, stretch induced ~40% neuronal death as determined by counts of MAP2-positive neurons (Fig. 3). Knockdown of PSD-95 had no effect on neuronal viability, and unlike the NMDA-mediated injury paradigm, PSD-95 knockdown did not protect neurons from stretch-induced injury (Fig. 3). These data suggest that the mechanisms that mediate injury caused by stretch and NMDA exposure differ.

Downregulation of PSD-95 prevents stretch-mediated decreases in dendrite branching

A second functional consequence of altering PSD-95 protein levels is decreased dendritic arborization.[25,26] Therefore, we performed Sholl analysis and simple dendrite assessment on cultured dissociated cortical neurons subjected to stretch injury. Stretch injury decreased Sholl curves and secondary and higher order dendrites and total dendrite length, number of branch points, and number of terminal points (Fig. 4). Because PSD-95 is involved in regulation of dendrite branching by binding to the microtubule +TIP binding proteins EB3[25,26] and APC,[27] we asked whether downregulation of PSD-95 can prevent these stretch injury-mediated decreases in dendrite branching. PSD-95 knockdown partially prevented stretch-mediated decreases in secondary dendrite number and total dendrite length post-injury (Fig. 4 D,G). However, it did not reverse decreases seen in the Sholl curve (Fig. 4 B). Although PSD-95 knockdown resulted in decreases in the number of higher order dendrites, total dendrite number, number of branch points, and terminal points (Fig. 4 E,F,H,I), stretch injury does not further induce decreases, suggesting that PSD-95 must be present for stretch injury to mediate insult to the arbor. Therefore, targeting PSD-95 knockdown after TBI may be a therapeutic strategy for restoring the dendritic arbor.

The second PDZ domain of PSD-95 is necessary for the regulation of dendritic arborization

With our data showing that PSD-95 is necessary for mediating changes to the dendritic arbor, we next identified the domain of PSD-95 that mediates the changes we observed in dendritic arborization from PSD-95 knockdown. It has been reported that

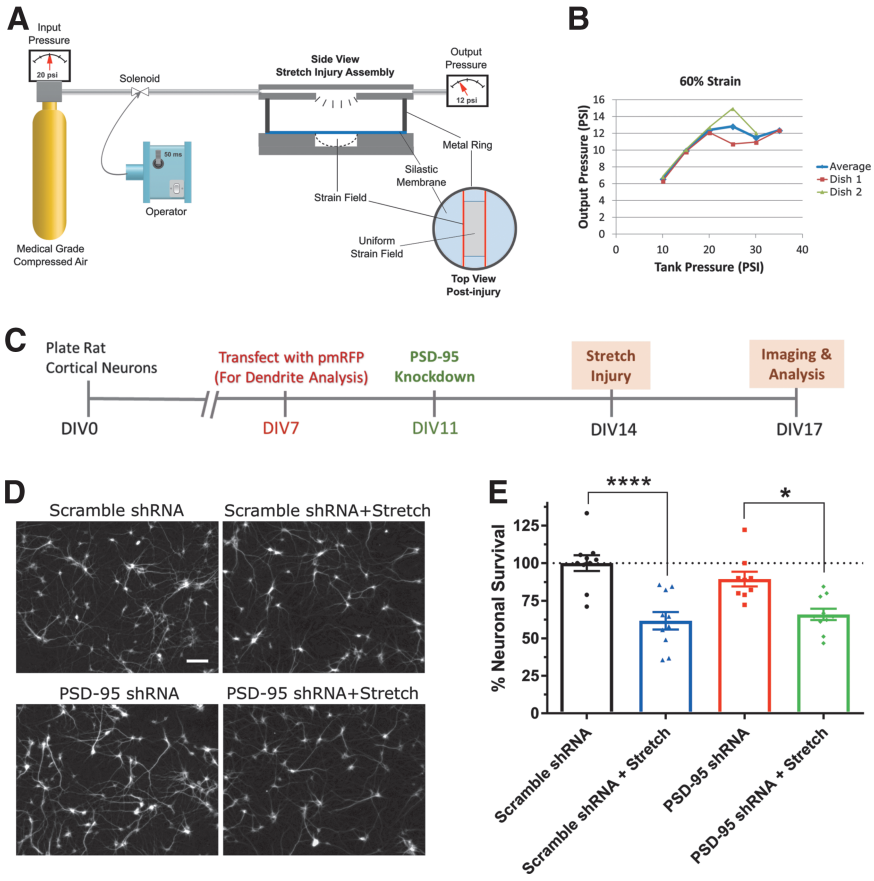

FIG. 3. Postsynaptic density 95 (PSD-95) knockdown does not prevent stretch injury-induced neuronal death. **(A)** Schematic of stretch injury device. **(B)** Data collected from the device, showing consistent output pressure of 12 psi for an applied pressure of 20 psi. **(C)** Experimental timeline for neuronal survival and dendrite branching analysis after stretch injury. **(D)** Representative images of MAP2-positive neurons for each condition. **(E)** Percentage of surviving neurons at 3 days after injury. $*p<0.05$; $****p<0.0001$ as determined by one way analysis of variance (ANOVA) followed by Tukey's multiple comparisons test. $n=10$ regions of interest (ROI) per condition of single independent experiment. Experiment was repeated three times. Error bars = SEM Scale bar = 100 μm.

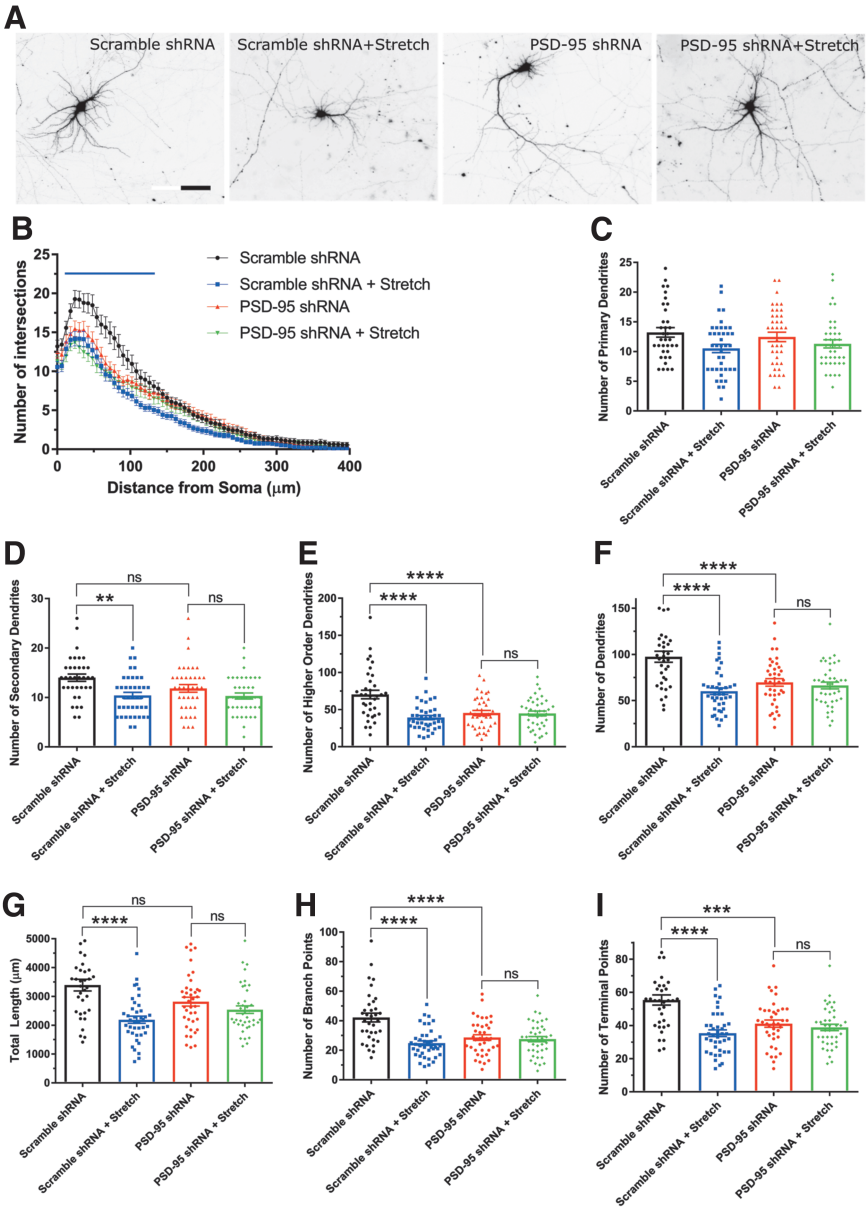

FIG. 4. Postsynaptic density 95 (PSD-95) knockdown prevents stretch injury-mediated decreases in dendrite branching. **(A)** Representative images of neurons expressing mRFP and transduced with virus encoding scramble or PSD-95 shRNA. Shown is the mRFP channel for single neuron dendrite analysis. **(B)** Sholl analysis of transfected neurons. Blue line indicates $*p < 0.05$ for control versus stretch injury for neurons transduced with virus for scrambled shRNA at distances 18– 132 μm away from soma as determined by two way analysis of variance (ANOVA) followed by Tukey's multiple comparisons test. **(C)** Neither stretch injury nor PSD-95 knockdown decreases primary dendrites. **(D)** PSD-95 knockdown prevents stretch-mediated decreases in secondary dendrite numbers. **(E)** PSD-95 knockdown decreases higher order dendrites, and stretch does not cause a further decrease. **(F)** PSD-95 knockdown decreases total dendrite numbers, and stretch does not cause a further decrease. **(G)** PSD-95 knockdown prevents stretch-mediated decreases in total dendrite length. **(H)** PSD-95 knockdown decreases number of dendrite branch points, and stretch does not cause a further decrease. **(I)** PSD-95 knockdown decreases the number of dendrite terminal points, and stretch does not cause a further decrease. $**p < 0.01$, $***p < 0.001$, and $****p < 0.0001$ as determined by one way ANOVA followed by Tukey's multiple comparisons test. $n = 35$–41 neurons. Error bars = SEM. Scale bar = 100 μm.

PSD-95 levels change in rat and mouse models of TBI,[49,50] and that excitatory scaffold networks mediate the downstream effects of TBI.[52] Specifically, two PSD-95 interactors, EB3[26,52] and APC,[27–29] regulate microtubule dynamics, a process involved in dendritic remodeling, an important component of recovery. We previously reported that the interaction between PSD-95 and EB3 regulates dendrite number; however, this interaction does not fully explain PSD-95-mediated decreases in dendrite number.[26] We also reported that the presence of the SH3 domain is needed for PSD-95-promoted decreases in dendrite branching.[26] To extend these studies and identify potential PSD-95 interactors that may regulate dendrite number after injury, we overexpressed PSD-95 and PSD-95 lacking PDZ1 (PSD-95ΔPDZ1), PDZ2 (PSD-95ΔPDZ2), or PDZ3 (PSD-95ΔPDZ3) in cultured hippocampal neurons from DIV

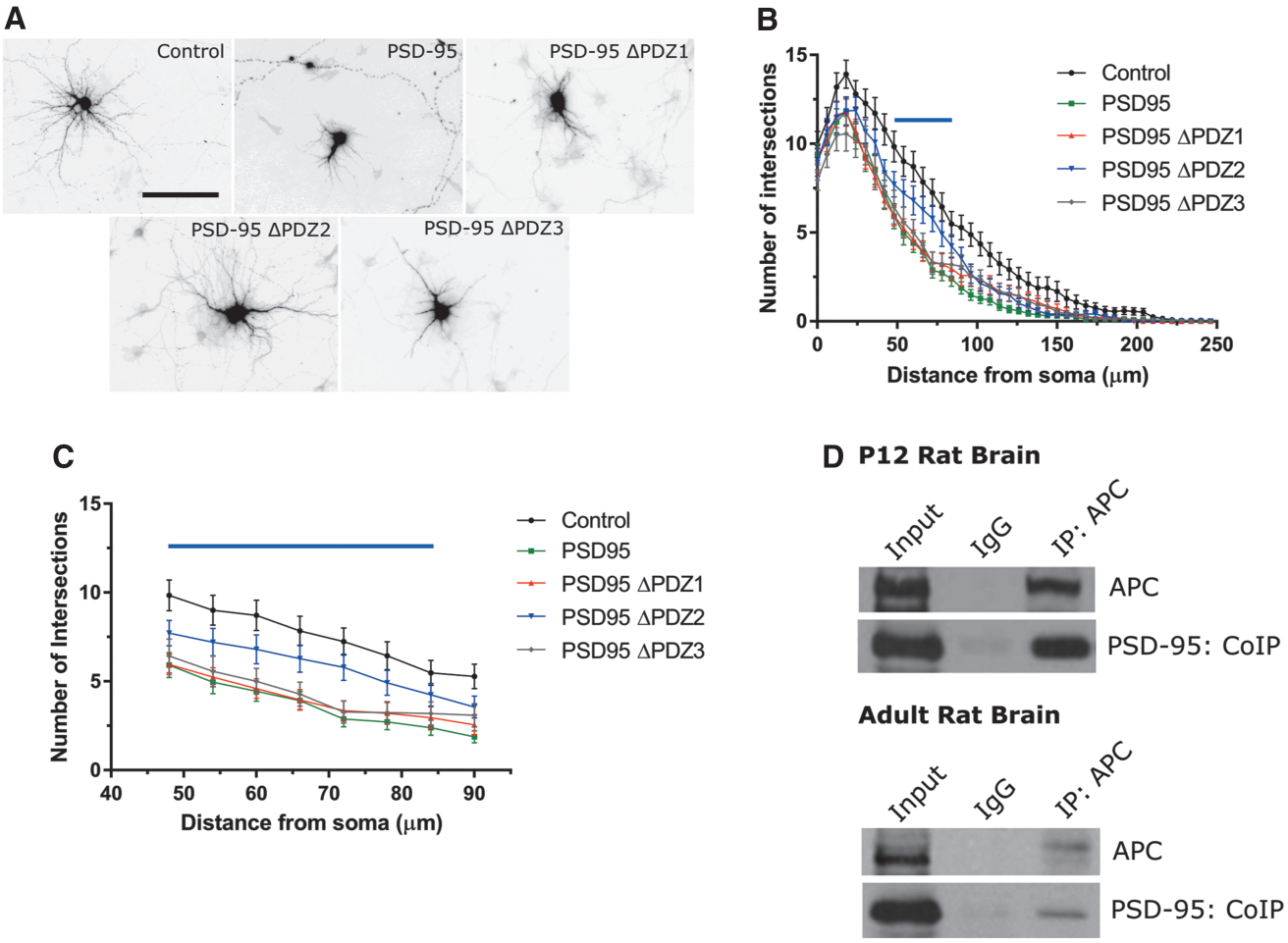

FIG. 5. The second PDZ domain is necessary for postsynaptic density 95 (PSD-95)-mediated decreases in dendritic arborization. **(A)** Representative images of neurons expressing mRFP (to elucidate morphology) and co-expressing green fluorescent protein (GFP), GFP-tagged PSD-95, PSD-95ΔPDZ1, PSD-95ΔPDZ2, or PSD-95ΔPDZ3. **(B,C)** Sholl analysis of neurons expressing the indicated proteins. Deletion of PDZ2 (PSD-95ΔPDZ2) attenuates PSD-95-mediated decreases in dendritic arborization for distances of 48–84 μm away from the soma, whereas deletion of PDZ1 and PDZ3 (PSD-95ΔPDZ1 and PSD-95ΔPDZ3) do not. Blue line indicates $p < 0.05$ for PSD-95 versus PSD-95ΔPDZ2 as determined by two way analysis of variance (ANOVA) followed by Tukey's multiple comparisons test. $n = 23$–25 neurons for each condition. Error bars = SEM. Scale bar = 100 μm. **(D)** Adenomatous polyposis coli (APC) co-immunoprecipitates with PSD-95 from developing (P12) and adult rat brain. APC was immunoprecipitated from whole brain lysate from adult or P12 rats. Precipitates were subjected to immunoblotting followed by Western blot analysis with an antibody against PSD-95. Input represents 2% of protein used for immunoprecipitation (IP).

7 to DIV 12. As expected, overexpression of PSD-95 reduced dendrite numbers (Fig. 5 A-C). When the second PDZ domain of PSD-95 was deleted, PSD-95 overexpression did not decrease dendrite branching to the levels seen with overexpression of intact PSD-95. Therefore, in addition to the SH3 domain, and the binding of EB3 to this domain,[26] PDZ2 interactors may play a role in regulating the dendritic arbor.

Because APC interacts with PSD-95 via its second PDZ domain,[27] and this interaction promotes microtubule bundling,[29] we confirmed that this interaction exists in the brain. Interestingly, co-IP experiments show that APC associates with PSD-95 to a greater degree in the developing rat brain (P12) when dendritogenesis is occurring than it does in the adult rat brain when dendritogenesis has stopped (Fig. 5 D). Therefore, based on the fact that the second domain of PSD-95 regulates dendrite morphology and APC binds to this region (and to EB3 independently of PSD-95[53]) and is involved in the regulation of microtubule dynamics, we performed experiments to assess whether interaction of PSD-95 with APC and EB3 is altered after injury.

Interaction with PSD-95 interactors, EB3, and APC, are altered in response to moderate CCI

Because we identified the SH3 and PDZ2 domains of PSD-95 as being essential for shaping the dendritic arbor, which is altered after injury, we next explored if brain trauma alters the association of PSD-95 with binding partners EB3 and APC. We immunoprecipitated PSD-95 to identify the relative association between PSD-95 and either EB3 or APC after injury. We observed that the levels of EB3 that co-immunoprecipitate with PSD-95 increased at 1 day and 7 days and the levels of co-immunoprecipitated APC increased at 1 day after moderate CCI (Fig. 1 A,B, right panels; Supplementary Fig. S1 [IgG control]). Similar to the fact that we did not observe changes to total levels of EB3 and APC post-injury,

there were no significant changes in the association of PSD-95 with either EB3 or APC at any time point following mild CCI. Total protein levels of PSD-95 and its interaction with APC and EB3 returned to control levels by 14 days post-CCI (Fig. 1 C). Our results demonstrate that PSD-95 and its interaction with APC and EB3 may be involved in post-injury response and that response mechanisms after mild and moderate TBI differ.

Discussion

In this study, we assessed how changes to PSD-95 and interaction with binding partners change after injury using both *in vitro* and *in vivo* models of TBI. Our *in vivo* data suggest that mild and moderate injury induce distinct pathways. Total levels of PSD-95 and its interaction with EB3 increase in the injured hippocampus at 1 and 7 days after moderate CCI, and interaction with APC increases at 1 day after moderate CCI. However, we did not observe significant change in either PSD-95 or its binding partners at any time point following mild CCI. Using an *in vitro* model of mechanical trauma to dissociated cortical neurons, we report that knockdown of PSD-95 does not promote neuronal survival but prevents changes to dendrites after stretch-induced injury *in vitro*. Taken together, our data suggest a role for PSD-95 and binding partners post-injury.

Our data are in contrast to those presented in previous studies showing a reduction of PSD-95 expression in the hippocampus[48,49,54,55] and the cortex[55] 1–7 days after CCI. The differences in data may be the result of a number of parameters. First, our study includes cortical tissue whereas the majority of previous reports studied the hippocampus. Second, we examined tissue after mild or moderate CCI, whereas the previous studies used a severe CCI model.[55] This difference in models is important, as differential effects of mild and moderate CCI on post-injury protein levels are observed here (Fig. 1) and in published work.[56,57] Further, different models, including rats[49,54] and mice[50,55] were used in the studies.

We observed high variability in co-IP of EB3 and APC with PSD-95 after moderate injury (Fig. 1). This may be because both APC[27] and EB3[25] bind to PSD-95, and APC and EB3 also directly bind to each other.[53] Therefore, co-immunoprecipitates of PSD-95 include the combination of the direct APC–PSD-95 and the indirect APC–EB3–PSD-95 interaction, each of which may be altered distinctly after injury.

How the interaction between PSD-95 and its binding partners may regulate the dendritic arbor after injury can been gleaned from past work from our group and that of others. We previously reported that PSD-95 binds to EB3 and sequesters EB3 from the +TIPs of microtubules, altering microtubule polarity, therefore resulting in decreased dendrite branching.[25,26] This suggests that early after mild injury, when higher levels of EB3 remain unbound to PSD-95, remodeling of dendrites can occur. In contrast, moderate injury promotes mechanisms that reduce dendrite branching and remodeling as EB3 is sequestered from microtubules. Further, there are reports that binding of PSD-95 to APC enhances microtubule bundling in COS-7 cells,[29] and this microtubule bundling with PSD-95 overexpression correlates with decreased dendrites.[25] Thus, the transient increase in the interaction between APC and PSD-95 at 1 day after moderate injury is also consistent with mechanisms that reduce dendrite branching and remodeling.

A

Injury	Total Levels			PSD-95 Interaction	
	PSD-95	APC	EB3	APC	EB3
1 day post-CCI (Moderate)	↑	-	-	↑	↑
7 days post-CCI (Moderate)	↑	-	-	-	↑
14 days post-CCI (Moderate)	-	-	-	-	-

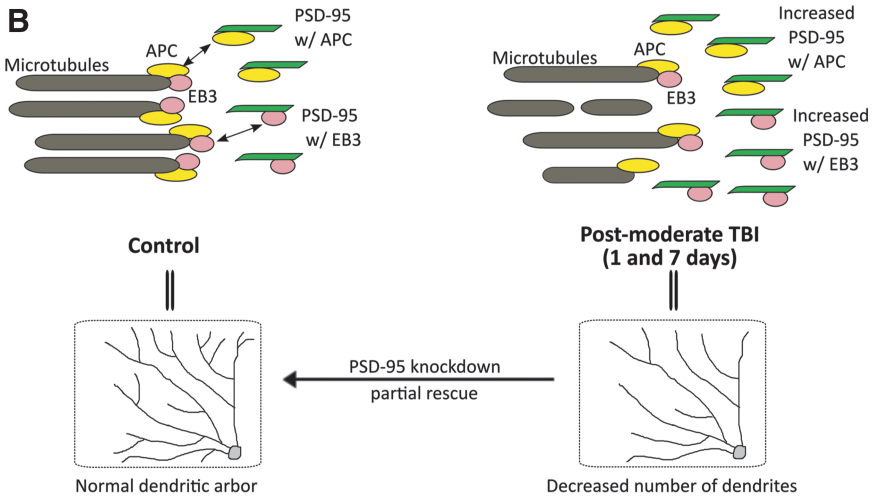

FIG. 6. Model of role of postsynaptic density 95 (PSD-95) and interactors after moderate controlled cortical impact (CCI). **(A)** Summary of findings. **(B)** Model showing increases in PSD-95 and interaction with adenomatous polyposis coli (APC) and end-binding protein 3 (EB3) after moderate CCI. Increased PSD-95 level results in decreased dendrite numbers, and increased PSD-95 interaction with APC and EB3 decreases APC and EB3 binding to +TIPs. This results in decreased dendrite dynamics and increased microtubule bundling, leading to decreased dendrite numbers. Knockdown of PSD-95 prevents changes to dendrites after stretch-induced injury by increasing free EB3 and APC, allowing them to bind to +TIPs of microtubules.

Collectively, moderate, but not mild, injury induces mechanisms that are detrimental to dendrite regrowth after injury. A model depicting these mechanisms is presented in Figure 6.

We have previously reported that knockdown of PSD-95 is neuroprotective against NMDA-induced excitotoxicity (secondary injury).[23] However, here we report that PSD-95 knockdown does not prevent mechanical stretch-induced injury (primary injury)-mediated neuronal death. These data suggest distinct mechanisms for primary versus secondary injury. Although both types of injury are mediated by the NMDA receptor, mechanotransduction, which occurs during primary injury, is mediated by NR1/NR2B NMDA receptors,[58,59] whereas overstimulation of multiple subunit-containing NMDA receptors can mediate neuronal death.[60,61] Similarly, we reported that knockdown of PSD-95 increases the number of secondary dendrites in immature neurons.[25] Here, we do not report an increase in proximal dendrites when PSD-95 is knocked down. This may be because in our previous study,[25] PSD-95 was knocked down and dendrites were assessed during the active branching period (by DIV 12), whereas in the current study, we knocked down and assessed dendrite numbers after the dendritic arbors had stabilized (DIV 17). Here, knockdown of PSD-95 decreased the number of higher order dendrites, total dendrite number, number of branch points, and terminal points. This is consistent with our previous report that PSD-95 knockdown results in decreased total dendrites and lengths because of a limiting reagent in the neuron.[25] Taken together, our published and current results suggest distinct roles for PSD-95 at different developmental time points; that is, when active dendritic branching occurs and when the arbor is stabilized, having implications for restoration of dendrites after injury.

Our study shows for the first time that stretch injury decreases dendritic arborization of surviving cortical neurons. Because TBI leads to acute dendritic degeneration,[14,55] stretch-induced injury can be used as an *in vitro* TBI model to study the effect of trauma on dendrite branching. Our PSD-95 knockdown studies show that PSD-95 is required for the stretch injury-mediated insult to the dendritic arborization and that knocking down PSD-95 is a therapeutic strategy for restoration of neural circuitry after TBI. However, because PSD-95 is an essential mediator of spinogenesis,[62] the timing of PSD-95 knockdown after injury is crucial for restoration of the dendritic arbor and allowance of spine reemergence and synapse stability.

Acknowledgments

This work was funded by the New Jersey Commission on Brain Injury Research grant # CBIR14IRG019 (to B.L.F. and D.F.M.). M.V.P. was supported in part by a pre-doctoral fellowship from the New Jersey Commission on Brain Injury Research # CBIR15-FEL009.

Author Disclosure Statement

No competing financial interests exist.

Supplementary Material

Supplementary Figure S1

References

1. Taylor, C.A., Bell, J.M., Breiding, M.J., and Xu, L. (2017). Traumatic brain injury-related emergency department visits, hospitalizations, and deaths – United States, 2007 and 2013. MMWR Surveill. Summ. 66, 1–16.
2. Cohen, J.S., Gioia, G., Atabaki, S., and Teach, S.J. (2009). Sports-related concussions in pediatrics. Curr. Opin. Pediatr. 21, 288–293.
3. Elder, G.A., and Cristian, A. (2009). Blast-related mild traumatic brain injury: mechanisms of injury and impact on clinical care. Mt. Sinai J. Med. 76, 111–118.
4. Ray, S., Dixon, C., and Banik, N. (2002). Molecular mechanisms in the pathogenesis of traumatic brain injury. Histol. Histopathol. 17, 1137–1152.
5. Mark, L.P., Prost, R.W., Ulmer, J.L., Smith, M.M., Daniels, D.L., Strottmann, J.M., Brown, W.D., and Hacein-Bey, L. (2001). Pictorial review of glutamate excitotoxicity: fundamental concepts for neuroimaging. Am. J. Neuroradiol. 22, 1813–1824.
6. Monnerie, H., Tang-Schomer, M.D., Iwata, A., Smith, D.H., Kim, H.A., and Le Roux, P.D. (2010). Dendritic alterations after dynamic axonal stretch injury in vitro. Exp. Neurol. 224, 415–423.
7. Levin, H.S., and Robertson, C.S. (2013). Mild traumatic brain injury in translation. J. Neurotrauma 30, 610–617.
8. Dikmen, S.S., Corrigan, J.D., Levin, H.S., Machamer, J., Stiers, W., and Weisskopf, M.G. (2009). Cognitive outcome following traumatic brain injury. J. Head Trauma Rehabil. 24, 430–438.
9. Marshall, L.F. (2000). Head injury: Recent past, present, and future. Neurosurg. 47, 546–561.
10. Prins, M., Greco, T., Alexander, D., and Giza, C.C. (2013). The pathophysiology of traumatic brain injury at a glance. Dis. Model. Mech. 6, 1307–1315.
11. Hill, C.S., Coleman, M.P., and Menon, D.K. (2016). Traumatic axonal injury: mechanisms and translational opportunities. Trends Neurosci. 39, 311–324.
12. Siedler, D.G., Chuah, M.I., Kirkcaldie, M.T., Vickers, J.C., and King, A.E. (2014). Diffuse axonal injury in brain trauma: insights from alterations in neurofilaments. Front. Cell Neurosci. 8, 429.
13. Johnson, V.E., Stewart, W., and Smith, D.H. (2013). Axonal pathology in traumatic brain injury. Exp. Neurol. 246, 35–43.
14. Gao, X., Deng, P., Xu, Z.C., and Chen, J. (2011). Moderate traumatic brain injury causes acute dendritic and synaptic degeneration in the hippocampal dentate gyrus. PloS One 6, e24566.
15. Cho, K.O., Hunt, C.A., and Kennedy, M.B. (1992). The rat brain postsynaptic density fraction contains a homolog of the Drosophila discs–large tumor suppressor protein. Neuron 9, 929–942.
16. Kistner, U., Wenzel, B.M., Veh, R.W., Cases-Langhoff, C., Garner, A.M., Appeltauer, U., Voss, B., Gundelfinger, E.D., and Garner, C.C. (1993). SAP90, a rat presynaptic protein related to the product of the Drosophila tumor suppressor gene dlg-A. J. Biol. Chem. 268, 4580–4583.
17. Kim, E., Niethammer, M., Rothschild, A., Jan, Y.N., and Sheng, M. (1995). Clustering of Shaker-type K+ channels by interaction with a family of membrane-associated guanylate kinases. Nature 378, 85–88.
18. Kornau, H.C., Schenker, L.T., Kennedy, M.B., and Seeburg, P.H. (1995). Domain interaction between NMDA receptor subunits and the postsynaptic density protein PSD-95. Science 269, 1737–1740.
19. Brenman, J.E., Chao, D.S., Gee, S.H., McGee, A.W., Craven, S.E., Santillano, D.R., Wu, Z., Huang, F., Xia, H., Peters, M.F., Froehner, S.C., and Bredt, D.S. (1996). Interaction of nitric oxide synthase with the postsynaptic density protein PSD-95 and alpha1-syntrophin mediated by PDZ domains. Cell 84, 757–767.
20. Kim, E., Cho, K.O., Rothschild, A., and Sheng, M. (1996). Heteromultimerization and NMDA receptor-clustering activity of Chapsyn-110, a member of the PSD-95 family of proteins. Neuron 17, 103–113.
21. Sattler, R., Xiong, Z., Lu, W.Y., Hafner, M., MacDonald, J.F., and Tymianski, M. (1999). Specific coupling of NMDA receptor activation to nitric oxide neurotoxicity by PSD-95 protein. Science 284, 1845–1848.
22. Yamada, Y., Chochi, Y., Takamiya, K., Sobue, K., and Inui, M. (1999). Modulation of the channel activity of the epsilon2/zeta1-subtype *N*-methyl-D-aspartate receptor by PSD-95. J. Biol. Chem. 274, 6647–6652.
23. Tseng, C.-Y., and Firestein, B.L. (2011). The role of PSD-95 and cypin in morphological changes in dendrites following sublethal NMDA exposure. J. Neurosci. 31, 15,468–15,480.
24. El-Husseini, A.E.-D., Schnell, E., Chetkovich, D.M., Nicoll, R.A., and Bredt, D.S. (2000). PSD-95 involvement in maturation of excitatory synapses. Science 290, 1364–1368.

25. Charych, E.I., Akum, B.F., Goldberg, J.S., Jornsten, R.J., Rongo, C., Zheng, J.Q., and Firestein, B.L. (2006). Activity-independent regulation of dendrite patterning by postsynaptic density protein PSD-95. J. Neurosci. 26, 10,164–10,176.
26. Sweet, E.S., Previtera, M.L., Fernandez, J.R., Charych, E.I., Tseng, C.Y., Kwon, M., Starovoytov, V., Zheng, J.Q., and Firestein, B.L. (2011). PSD-95 alters microtubule dynamics via an association with EB3. J. Neurosci. 31, 1038–1047.
27. Yanai, H., Satoh, K., Matsumine, A., and Akiyama, T. (2000). The colorectal tumour suppressor APC is present in the NMDA-receptor-PSD-95 complex in the brain. Genes Cells 5, 815–822.
28. Munemitsu, S., Souza, B., Müller, O., Albert, I., Rubinfeld, B., and Polakis, P. (1994). The APC gene product associates with microtubules in vivo and promotes their assembly in vitro. Cancer Res. 54, 3676–3681.
29. Takamori, N., Shimomura, A., and Senda, T. (2006). Microtubule-bundling activity of APC is stimulated by interaction with PSD-95. Neurosci. Lett. 403, 68–72.
30. Weiner, A.T., Lanz, M.C., Goetschius, D.J., Hancock, W.O., and Rolls, M.M. (2016). Kinesin-2 and Apc function at dendrite branch points to resolve microtubule collisions. Cytoskeleton (Hoboken) 73, 35–44.
31. Votin, V., Nelson, W.J., and Barth, A.I. (2005). Neurite outgrowth involves adenomatous polyposis coli protein and beta-catenin. J. Cell Sci. 118, 5699–5708.
32. Koester, M.P., Muller, O., and Pollerberg, G.E. (2007). Adenomatous polyposis coli is differentially distributed in growth cones and modulates their steering. J. Neurosci. 27, 12590–12600.
33. Gartner, A., Huang, X., and Hall, A. (2006). Neuronal polarity is regulated by glycogen synthase kinase-3 (GSK-3beta) independently of Akt/PKB serine phosphorylation. J. Cell Sci. 119, 3927–3934.
34. Choo, A.M., Miller, W.J., Chen, Y.-C., Nibley, P., Patel, T.P., Goletiani, C., Morrison III, B., Kutzing, M.K., Firestein, B.L., and Sul, J.-Y. (2013). Antagonism of purinergic signalling improves recovery from traumatic brain injury. Brain 136, 65–80.
35. Chen, Y., Mao, H., Yang, K.H., Abel, T., and Meaney, D.F. (2014). A modified controlled cortical impact technique to model mild traumatic brain injury mechanics in mice. Front. Neurol. 5, 100.
36. Patel, M.V., Swiatkowski, P., Kwon, M., Rodriguez, A.R., Campagno, K., and Firestein, B.L. (2018). A novel short isoform of cytosolic PSD-95 interactor (Cypin) regulates neuronal development. Mol. Neurobiol. 55, 6269–6281.
37. Kutzing, M.K., Luo, V., and Firestein, B.L. (2011). Measurement of synchronous activity by microelectrode arrays uncovers differential effects of sublethal and lethal glutamate concentrations on cortical neurons. Ann. Biomed. Eng. 39, 2252–2262.
38. Kutzing, M.K., Luo, V., and Firestein, B.L. (2012). Protection from glutamate-induced excitotoxicity by memantine. Ann. Biomed. Eng. 40, 1170–1181.
39. Hernandez, K., Swiatkowski, P., Patel, M.V., Liang, C., Dudzinski, N.R., Brzustowicz, L.M., and Firestein, B.L. (2016). Overexpression of isoforms of nitric oxide synthase 1 adaptor protein, encoded by a risk gene for schizophrenia, alters actin dynamics and synaptic function. Front. Cell Neurosci. 10, 6.
40. Svane, K.C., Asis, E.K., Omelchenko, A., Kunnath, A.J., Brzustowicz, L.M., Silverstein, S.M., and Firestein, B.L. (2018). d-Serine administration affects nitric oxide synthase 1 adaptor protein and DISC1 expression in sex-specific manner. Mol. Cell Neurosci. 89, 20–32.
41. Akum, B.F., Chen, M., Gunderson, S.I., Riefler, G.M., Scerri-Hansen, M.M., and Firestein, B.L. (2004). Cypin regulates dendrite patterning in hippocampal neurons by promoting microtubule assembly. Nat. Neurosci. 7, 145–152.
42. Lusardi, T.A., Wolf, J.A., Putt, M.E., Smith, D.H., and Meaney, D.F. (2004). Effect of acute calcium influx after mechanical stretch injury in vitro on the viability of hippocampal neurons. J. Neurotrauma 21, 61–72.
43. Mesfin, M.N., von Reyn, C.R., Mott, R.E., Putt, M.E., and Meaney, D.F. (2012). In vitro stretch injury induces time-and severity-dependent alterations of STEP phosphorylation and proteolysis in neurons. J. Neurotrauma 29, 1982–1998.
44. Spaethling, J., Le, L., and Meaney, D.F. (2012). NMDA receptor mediated phosphorylation of GluR1 subunits contributes to the appearance of calcium-permeable AMPA receptors after mechanical stretch injury. Neurobiol. Dis. 46, 646–654.
45. Mendenhall, A., Lesnik, J., Mukherjee, C., Antes, T., and Sengupta, R. (2012). Packaging HIV- or FIV-based lentivector expression constructs and transduction of VSV-G pseudotyped viral particles. J. Vis. Exp. 62, e3171.
46. Kutzing, M.K., Langhammer, C.G., Luo, V., Lakdawala, H., and Firestein, B.L. (2010). Automated Sholl analysis of digitized neuronal morphology at multiple scales. J. Vis. Exp. 45, 2354.
47. O'Neill, K.M., Akum, B.F., Dhawan, S.T., Kwon, M., Langhammer, C.G., and Firestein, B.L. (2015). Assessing effects on dendritic arborization using novel Sholl analyses. Front. Cell Neurosci. 9, 285.
48. Nortje, J., and Menon, D.K. (2004). Traumatic brain injury: physiology, mechanisms, and outcome. Curr. Opin. Neurol. 17, 711–718.
49. Ansari, M.A., Roberts, K.N. and Scheff, S.W. (2008). A time course of contusion-induced oxidative stress and synaptic proteins in cortex in a rat model of TBI. J. Neurotrauma 25, 513–526.
50. Wakade, C., Sukumari-Ramesh, S., Laird, M.D., Dhandapani, K.M., and Vender, J.R. (2010). Delayed reduction in hippocampal postsynaptic density protein-95 expression temporally correlates with cognitive dysfunction following controlled cortical impact in mice. J. Neurosurg. 113, 1195–1201.
51. Luo, P., Fei, F., Zhang, L., Qu, Y., and Fei, Z. (2011). The role of glutamate receptors in traumatic brain injury: implications for postsynaptic density in pathophysiology. Brain Res. Bull. 85, 313–320.
52. Sweet, E.S., Tseng, C.Y. and Firestein, B.L. (2011). To branch or not to branch: how PSD-95 regulates dendrites and spines. Bioarchitecture 1, 69–73.
53. Nakagawa, H., Koyama, K., Murata, Y., Morito, M., Akiyama, T., and Nakamura, Y. (2000). EB3, a novel member of the EB1 family preferentially expressed in the central nervous system, binds to a CNS-specific APC homologue. Oncogene 19, 210–216.
54. Ansari, M.A., Roberts, K.N., and Scheff, S.W. (2008). Oxidative stress and modification of synaptic proteins in hippocampus after traumatic brain injury. Free Radic. Biol. Med. 45, 443–452.
55. Wang, C.F., Zhao, C.C., Jiang, G., Gu, X., Feng, J.F., and Jiang, J.Y. (2016). The role of posttraumatic hypothermia in preventing dendrite degeneration and spine loss after severe traumatic brain injury. Sci. Rep. 6, 37063.
56. Yu, S., Kaneko, Y., Bae, E., Stahl, C.E., Wang, Y., van Loveren, H., Sanberg, P.R., and Borlongan, C.V. (2009). Severity of controlled cortical impact traumatic brain injury in rats and mice dictates degree of behavioral deficits. Brain Res. 1287, 157–163.
57. Swiatkowski, P., Sewell, E., Sweet, E.S., Dickson, S., Swanson, R.A., McEwan, S.A., Cuccolo, N., McDonnell, M.E., Patel, M.V., Varghese, N., Morrison, B., Reitz, A.B., Meaney, D.F., and Firestein, B.L. (2018). Cypin: A novel target for traumatic brain injury. Neurobiol. Dis. 119, 13–25.
58. Singh, P., Doshi, S., Spaethling, J.M., Hockenberry, A.J., Patel, T.P., Geddes-Klein, D.M., Lynch, D.R., and Meaney, D.F. (2012). *N*-methyl-D-aspartate receptor mechanosensitivity is governed by C terminus of NR2B subunit. J. Biol. Chem. 287, 4348–4359.
59. Spaethling, J., Le, L., and Meaney, D.F. (2012). NMDA receptor mediated phosphorylation of GluR1 subunits contributes to the appearance of calcium-permeable AMPA receptors after mechanical stretch injury. Neurobiol. Dis. 46, 646–654.
60. Rameau, G.A., Akaneya, Y., Chiu, L., and Ziff, E.B. (2000). Role of NMDA receptor functional domains in excitatory cell death. Neuropharmacology 39, 2255–2266.
61. Sattler, R., and Tymianski, M. (2001). Molecular mechanisms of glutamate receptor-mediated excitotoxic neuronal cell death. Mol. Neurobiol. 24, 107–129.
62. El-Husseini, A.E., Schnell, E., Chetkovich, D.M., Nicoll, R.A., and Bredt, D.S. (2000). PSD-95 involvement in maturation of excitatory synapses. Science 290, 1364–1368.

Address correpondence to:
Bonnie L. Firestein, PhD
Department of Cell Biology and Neuroscience
Rutgers University
604 Allison Road
Piscataway, NJ 08854-8082

E-mail: firestein@biology.rutgers.edu